--- C U M U L A T I V E H A B I L I T A T I O N ---

On the topic:

SYNTHESIS AND PHYSICAL-CHEMICAL CHARACTERIZATION OF INNOVATIVE FOAM MATERIALS FROM WASTE RAW MATERIALS

Dr. Eng. Nicolai B. Jordanov,

Institute for Physical Chemistry, Bulgarian Academy of Sciences, IPC-BAS,

Department of Phase Formation, Crystalline and Amorphous Materials,

1113-Sofia

njordanov@ipc.bas.bg

I. Introduction.

98 percent air—or, expressed with other words, a foam material. In modern materials science, foams are difficult to classify as a single category, as they can be organic or inorganic by nature. They may also possess a crystalline, glassy-crystalline, or amorphous structure. They can exhibit a wide range of mechanical, insulating, and thermal properties. Furthermore, they can be produced via chemical or physical processes at either room temperature or at temperatures exceeding 1000°C. Most importantly, however, they are significantly lighter compared to the dense crystalline, glassy, or sintered materials and consist of one or more size populations of numerous thin-walled bubbles; these are formed during solidification through gas evolution within a viscoelastic medium or via vigorous stirring—either with or without the presence of surfactants (i.e. surface-active agents). Depending on the chemical mechanism of their formation, these closed

bubbles may contain various gases—such as oxygen, carbon dioxide, etc.—rather than merely atmospheric air (which is actually less common).

The content of the closed gas phase can vary; a typical range for a high-quality foam material is 75–98 vol. %. These materials are characterized by thermal and acoustic insulation properties, as well as chemical and water resistance.

Their surface can be smoothly glazed—offering an attractive appearance and fully closed pores—or adhesively bonded to another material to form a composite sandwich structure, a configuration highly sought after in the modern construction industry. The synthesis of sintered glass-ceramics depends on the interplay between viscous sintering and crystallization, whereas the production of glass-ceramic foams relies on the balance between apparent viscous sintering and gas evolution [1].

Gas evolution typically depends on oxidation or decomposition reactions involving modifying compounds during the foaming of glass-ceramics. Oxidation reactions involve the release of COx gases from carbon-containing compounds—such as carbon black, graphite, silicon carbide (SiC), and organic substances—as they react with atmospheric oxygen.

Typical decomposition reactions include those involving carbonates or sulfates, resulting in the release of CO_2 or SOx [1, 2]. A special case arises when the parent glass contains transition metal oxides (referred to as conditional glass-forming modifiers)—such as iron or manganese oxides—that undergo a transition from a higher to a lower oxidation state, accompanied by the release of oxygen gas. This is the specific scenario addressed in the present study.

The production of glass-ceramics from iron-rich metallurgical slag, for instance, can be halted at the stage of obtaining merely well-sintered glass-ceramics, or continued at any time to the glass-ceramic foam stage (in this specific case, for example, starting from an iron-rich base frit).

A highly contemporary trend today is the production of advanced foam materials utilizing a high percentage of waste raw materials, recycled into products with high added value and a low carbon footprint. In the following pages, I summarize the research I have conducted in this field of modern materials science—work carried out over the past six years that has culminated in this habilitation.

II. Sintering and crystallization.

The sintering of glass-ceramics is a typical example of induced structural densification in a solid sample. This process is triggered by density variations within the material's volume. It is the initial step (aside from any potential concurrent oxidation process) occurring during the formation of a new glass-ceramic material—a step that can be determined, for instance, via linear thermal scanning. The degree of densification is one of the most important characteristics of sintered glass-ceramics. It is largely determined by the particle size distribution, the crystallization ability (crystallization tendency) of the parent glass, and the heating rate of the compacted powder sample. A high crystallization trend can inhibit sintering, because the greater the tendency to crystallize, the lower the sinterability—and vice versa.

It is well known that the sinterability of vitreous powders can be significantly improved by using finer glass fractions and/or higher constant linear heating rates [1, 2]. Consequently, it can be concluded—and indeed this is the case—that both processes must be carefully balanced to successfully produce a truly high-quality material with enhanced properties. This means that both extremes—minimal or maximal crystallization of the glass-ceramic—must be avoided. The crystalline structure determines the material's stability and durability. Conversely, however, a variant with higher crystallinity cannot be sintered. Current understanding holds that both the sintering and crystallization processes occur within the same temperature range. For the purposes of the theoretical description, however, it is assumed that the sintering stage precedes the crystallization stage. In reality, sintering ceases once a certain critical percentage of crystalline phases has formed.

The apparent viscosity of the glass-ceramic is of crucial importance here. Its value must be maintained within a range that allows for structural expansion while temporarily preventing the formation and propagation of open porosity.

In the case under study, foaming is determined by the formation and distribution of a population of closed pores within the material's volume, resulting from the release of gas molecules (most commonly oxygen) during the high-temperature partial reduction of certain oxides from a higher to a lower oxidation state. These are most frequently iron [3] and manganese [4] oxides.

The high-temperature foaming range indicates that the gas formation mechanism is directly linked to oxygen release resulting from the reversible partial

reduction of Fe(III) and Mn(IV) [4, 5]. Furthermore, the presence of naturally occurring iron and manganese oxides in sufficient quantities within the base glass frit represents the most favorable scenario, as there is no need for the foaming process to be artificially or additionally catalyzed. Thus, an inorganic material is formed through autocatalytic foaming.

Over the past few decades, research has successfully continued on bulk glass-ceramics, sintered glass-ceramics, and ceramics or glass-ceramic foams derived from various slags and other metallurgical residues.

For instance, a glass-ceramic has been developed from Turkish blast-furnace slag using 3 and 5 wt. % TiO_2 as a nucleating agent [6]. A similar material was obtained by mixing 57 wt. % blast-furnace slag with quartz sand, dolomite, limestone, and clay [7]. In this study, Cr_2O_3, TiO_2, CaF_2, and LiF additives were used to enhance bulk crystallization capability. It was determined that Cr_2O_3 and TiO_2 act as more effective nucleating agents than LiF and CaF_2, and that their addition results in the formation of a fine-grained microstructure. Other glass-ceramics produced from iron waste and slag are used as architectural materials and in the chemical industry in China [8].

III. Experimental.

My research began with the task of elucidating the influence of the atmosphere on the high-temperature autocatalytic foaming process in thermally sintered glass-ceramic viscoelastic bodies—conducted *in-situ* within the working chamber of a contactless optical dilatometer combined with a high-temperature

heating microscope (EXPERT LAB SERVICE HSS-1400, Modena, Italy; collectively referred to here as the thermo-optical system, TOS).

Given that we deliberately employ a chemical "switch"—the reversible partial reduction of the Fe^{2+}/Fe^{3+} (ferro/ferri) oxide redox couple—during the synthesis of sintered glass-ceramic foams, it was hypothesized that the presence or absence of an oxidizing or reducing agent in the synthesis atmosphere would be of paramount importance to the thermal synthesis process. To this end, it was necessary to arrange for the design and fabrication of a sealed vessel capable of housing the entire TOS assembly and allowing the enclosed volume to be conditioned (purged and pressurized) with either argon gas or air, in order to determine the effect of the atmosphere on the foaming process of inorganic, iron-containing glassy-crystalline materials. As part of a newly awarded post-doctoral project funded by the Ministry of Education and Science of the Republic of Bulgaria, we constructed a low-cost vessel that we dubbed the "argon box." We were now able to experiment with the synthesis atmosphere, and results were not long in coming; unequivocal and technologically significant effects were observed.

For the purposes of the present experiments with sintered materials and foams, slag from the Helwan iron and steel company in the Cairo Governorate, Egypt (with an annual slag production capacity of 30 kt), was used to synthesize the samples under investigation. This slag is relatively poor in glass-forming constituents (SiO_2 and Al_2O_3); therefore, it had to be enriched with silicon dioxide by mixing 70 wt. % slag with 30 wt. % industrial sand.

The initial 150 g batch was melted in corundum crucibles using an electric furnace. After a 2-hour hold at 1450°C, the resulting homogeneous melt was quenched in water to produce a dark-brown glass frit. The resulting glass frit was crushed, ground several times in a planetary mill FRITSCH (Germany) for 10 minutes, and sieved to a particle size of less than 75 microns using a CISA (Spain) digitally programmed sieving machine.

The studies were conducted using the TOS setup. Latter has become an established laboratory method in recent years, as it has proven to be reliable and rapid, and is already being used by many research groups worldwide [9, 10].

The sintering behavior of all glass-ceramic samples was investigated using optical dilatometry (ODM), a method that enables measurements with very high precision. This is primarily due to the absence of mechanical pressure in the system, unlike in conventional contact dilatometers. Instead, the optical dilatometer employs a monochromatic optical setup utilizing two horizontally aligned video cameras that provide high magnification and high resolution. Standard measurements included a 30-minute holding time at 950 °C in air or argon.

A small amount of 7 wt. % aqueous solution of polyvinyl alcohol (PVA) is added to the sintered glass powder to form a sticky granular mass, which is then mechanically homogenized and placed into a 50 × 5 × 3 mm mold. Series of samples with identical shapes are prepared by freely (and loosely) filling the material into the pressing mold. Subsequently, by applying a uniaxial pressure of 40 MPa using a NANNETTI (Italy) hydraulic press, samples with nearly identical dimensions and densities—characterized by enhanced green strength and reduced

porosity—are prepared. Subsequently, a step involving the burnout of the organic binder at 270°C is required to remove the binding agent (e.g., PVA) before proceeding with the heat treatment processes. Burn-out can be carried out in the furnace, separately, or as an initial programmed step preceding the oxidation, sintering, and foaming stages.

The thermal behavior of the sintered samples in air and argon up to 1300 °C was investigated and analyzed using the optical dilatometry (ODM) method. While the samples used for ODM measurements had a standard parallelepiped shape (as described above), the samples used for heating microscopy (HM) measurements differed; they consisted of standard upright mini-cylinders with a height of 3 mm.

Furthermore, sample foaming trends were investigated by performing measurements both isothermally, with a holding time of 30 minutes (e.g., at 950 °C for simultaneous oxidation and sintering, and at 1100 °C to initiate foaming), and non-isothermally (using constant linear thermal scans with heating rates up to 40 ^{o}C min^{-1}). Typically, such thermal scans were conducted at heating rates of 20 °C min^{-1}.

During all measurements, the TOS instrument was mounted in a sealed aluminum box (designed and manufactured in the mechanical workshop of IPC-BAS Sofia), which enabled measurements in a controlled environment. The chamber of the box can be purged with dry argon gas if necessary. This setup allows for the continuous maintenance of an argon overpressure of ~10–15 mbar throughout the entire synthesis process, as well as optical measurement of thermal changes in the sample structure. This is achieved using a precision YOKOGAWA

(Japan) rotameter for manual control of the gas flow into the sample chamber and a high-precision PROFIMESS (Germany) digital pressure gauge with a ceramic diaphragm for comprehensive monitoring of the gas pressure.

To the best of the authors' knowledge, such a laboratory experimental setup—a combined TOS system installed in a sealed vessel for investigating the sintering and foaming behavior of iron-rich glass-ceramics in various atmospheres—is unique in Southeast Europe and was likely used for the first time in this context here (in 2019).

Scanning electron microscopy (SEM) was used to analyze the structure of the sintered glass-ceramics by imaging both the fracture surfaces and the sample surfaces. A JEOL 6390 instrument (Japan) was employed. To ensure electrical conductivity, all samples were coated with gold using a vapor deposition technique.

3D X-ray micro-computed tomography (μCT) was used for the comprehensive scanning of the glass-ceramic foams. The tomographic measurements were performed using a BRUKER SKYSCAN 1272 X-ray micro-CT scanner (Germany), which employs a cone-beam geometry. The following settings were applied: X-ray tube voltage of 70 kV, current of 142 mA, and a 0.11 mm Cu filter. The voxel (3D pixel) size was 1 μm, and the optical magnification was 7.4. A typical 360° scan took 21 hours and 27 minutes.

The 3D image reconstruction was performed using the commercial software InstaRecon. The phase composition of the sintered glass-ceramic foams was determined by X-ray diffraction (XRD) using a Panalytical Empyrean spectrometer (USA).

IV. Summary of results.

As previously stated, the innovative aspect of the present research—beyond the use of the sinter-crystallization method for the synthesis and production of sintered glass-ceramics and/or glass-ceramic foams—lies in the use of a controlled atmosphere during the synthesis of sintered glass-ceramics, specifically extending this to the production stage of glass-ceramic foams.

Figure 1 presents a comparative graphical representation—along with images taken at the respective characteristic temperatures—of the shape change observed during real-time *in-situ* imaging of two glass-ceramic samples synthesized in air or in argon atmosphere.

Up to temperatures of approx. 1050°C, the thermal behavior of the two types is quite similar. Both samples undergo similar densification during the low-temperature sintering interval. At higher temperatures, however, the iron-rich glass-ceramic materials, when heated in different atmospheres (air or inert), exhibit completely

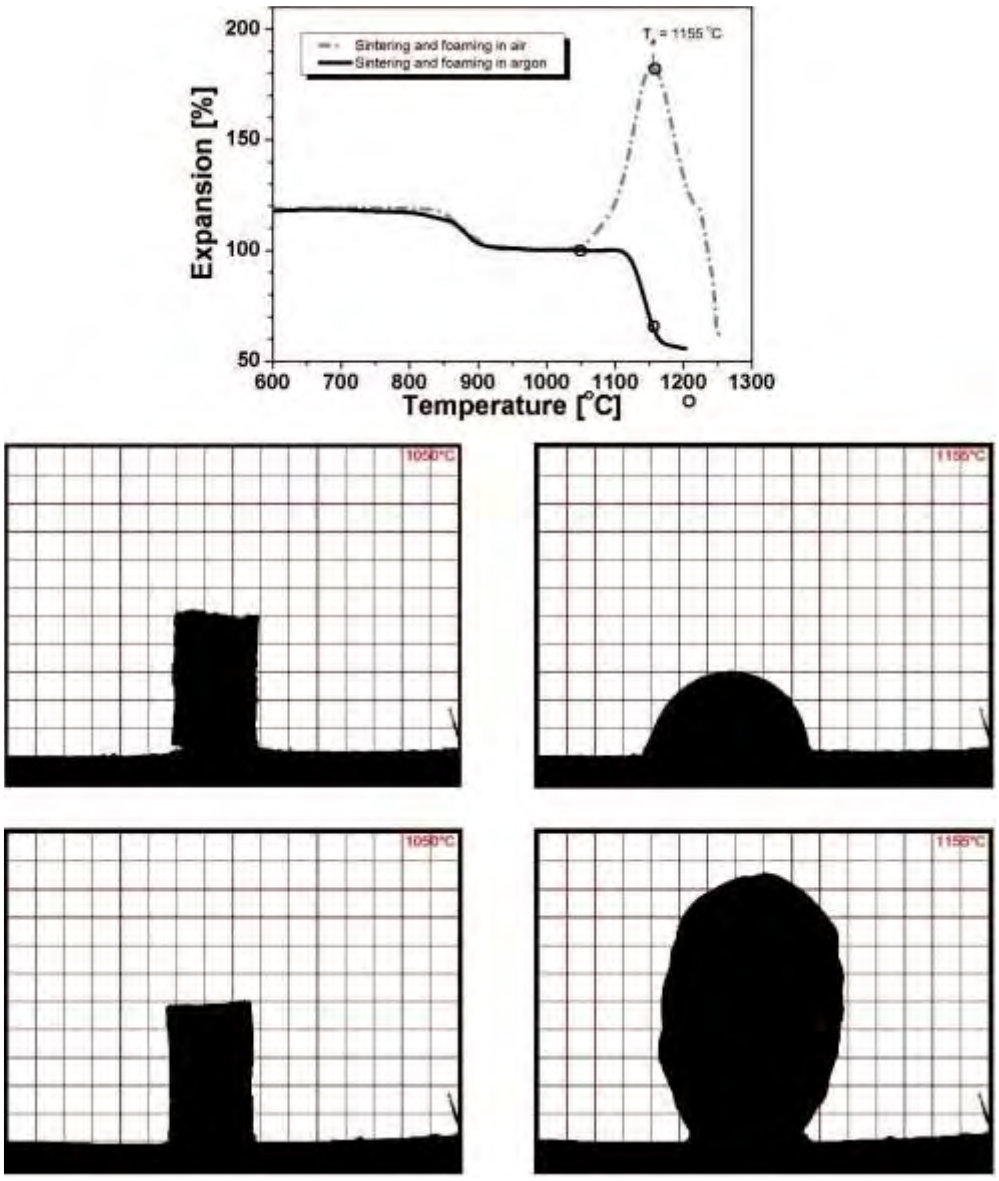


Figure 1. Sintering and expansion curves during the in-situ synthesis of glass-ceramic foam in the heating chamber of HM in an air or argon atmosphere.

different thermal behavior compared to one another when subjected to a similar subsequent heat treatment.

In the case of a sample sintered in argon, further heating of the material leads to melting (e.g., hemispherical slumping at 1155°C). However, the sample sintered in air begins to expand in volume during heat treatment above 1050°C; at the same reference temperature of 1155°C, it exhibits maximum structural expansion driven by gas evolution—specifically, foaming throughout the volume of the newly formed material. This difference in the thermal behavior of the two samples is primarily due to differences in the viscosity values of the respective materials. The phenomena described above are entirely determined by the equilibrium state of the Fe(II) ↔ Fe(III) redox couple, in the sense that an inert atmosphere (e.g., argon) maintains the equilibrium shifted maximally to the left (oxidation is inhibited [11]), whereas an air atmosphere keeps the Fe(II)/Fe(III) ratio at a minimum value—i.e., the equilibrium is shifted to the right.

3D X-ray tomographic analysis was used to investigate the entire bulk structure of the newly formed foam material. Figure 2a (left) shows a false-color 3D surface reconstruction and the volume obtained via tomographic scanning of an iron-rich glass-ceramic foam synthesized in air.

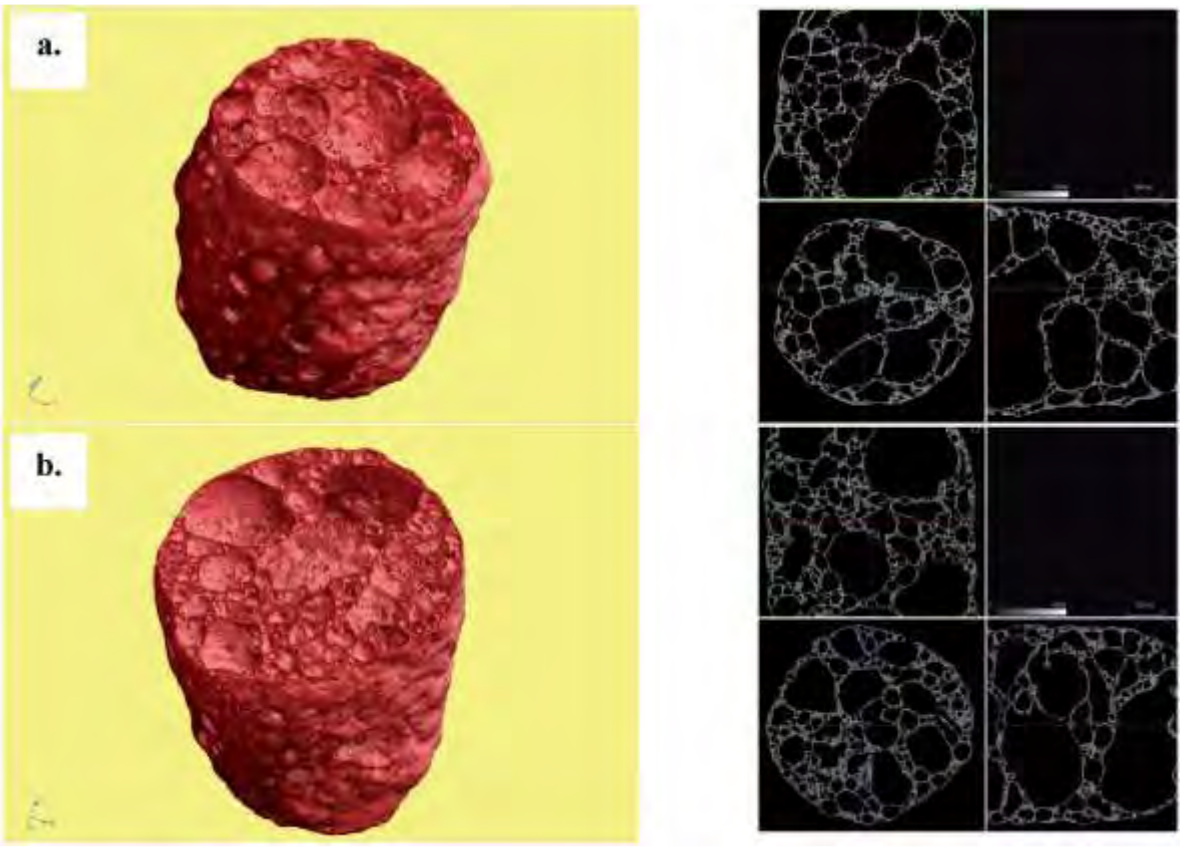


Figure 2. 3D reconstruction of the volume of glass-ceramic samples:

a. synthesis in air; **b.** synthesis in argon.

Visual observations and the conducted image analyses clearly indicate that the porosity within the volume of both samples is predominantly of the closed-cell type, amounting to approximately 80–85 vol. % for both varieties. It is also evident that the sample walls are rich in pores. Another interesting characteristic is that the closed cells of the variety foamed in air are larger than the cells within the volume of the sample foamed in argon. Furthermore, the wall thickness in the sample

synthesized in air is, on average, lower than the wall thickness in the glass-ceramic foam material obtained in an argon atmosphere.

It was determined that an initial thermal oxidation step is necessary to achieve effective foaming at higher temperatures. Figure 3 shows the peak foaming characteristics on the volume expansion curve taken by HM: with a programmed oxidation step (Fig. 3a) and without such a step (Fig. 3b).

At a high heating rate of 40 °C min^{-1}, the oxidized sample exhibits a maximum expansion of 737% for the sintered body, whereas the expansion is approximately 10% lower in the case without pre-oxidation.

At the same time, due to the longer oxidation time available in the case with the lower heating rate of 5 °C min-1, both curves show a similar bloating tendency.

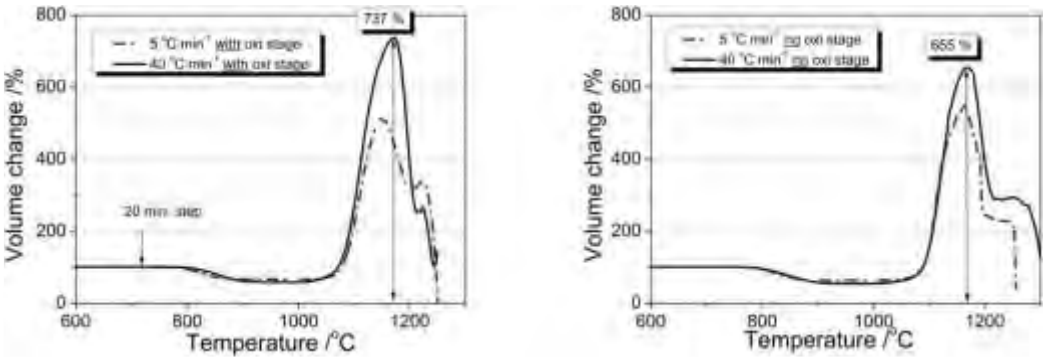


Figure 3. Peak foaming values for glass-ceramic samples with a programmed oxidation step (**left**) and without one (**right**), at two linear heating rates.

On the contrary, at high rates of at a heating rate of 40 °C min^{-1}, the available time for oxidation is insufficient, and introducing a preliminary isothermal oxidation

step offers a significant advantage. Furthermore, the crystallization process is not yet complete. The results obtained here regarding improved foaming with increased heating rates confirm our previous findings [12, 13].

For instance, figure 4 presents the overall graphical representation of the isothermal synthesis of glass-ceramic foams employed here, involving three isotherms at 1100, 1120, and 1150 °C (with a 20-minute hold at each of the three working isotherms and a 15-minute hold at each preliminary oxidation stage). The experimental temperatures were selected through a graphical analysis of linear heating curves—such as those shown in Fig. 1—which revealed the onset of the foaming process at 1100 °C, as well as intermediate and peak characteristics at 1120 and 1150 °C, respectively.

Thermal oxidation occurs near the glass transition temperature (Tg) of 720°C. At the isotherm of 1100°C, foaming is incomplete due to higher apparent viscosity. In the case of the 1120°C isotherm, foaming is more pronounced and intense than in the first curve.

At the 1150°C isotherm, the foaming process is faster and concludes earlier. However, due to the lower viscosity, sample shrinkage is observed—occurring both during the holding stage and during cooling. Consequently, both the final porosity and the final expansion are lower than those of the sample processed at 1120°C.

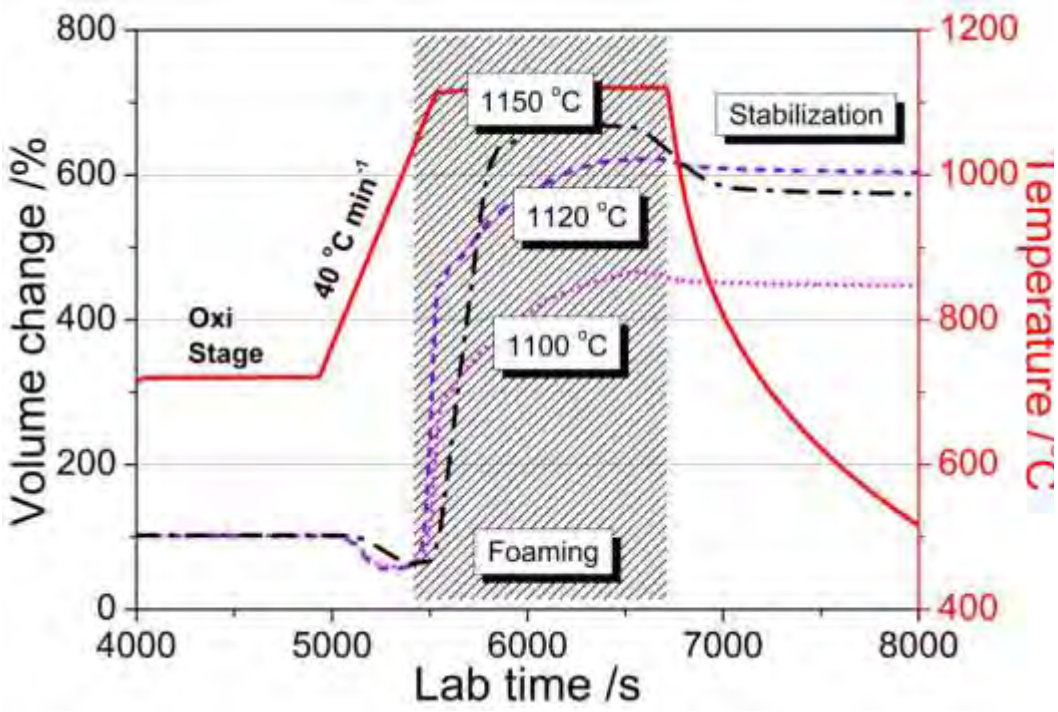


Figure 4. Sintering curves at three processing isotherms for the synthesis of glass-ceramic foam materials.

Figure 5 shows a SEM image of the fracture surface of the resulting foam material. Two modes of bubble distribution (bimodal)—within the walls and within the bulk of the analyzed sample—can be clearly distinguished. This bimodal distribution is typically observed in this specific case of iron oxide reduction, confirming our previous results [13]. The inset in figure 3 shows a true-color digital photograph of the foam produced *in-situ*.

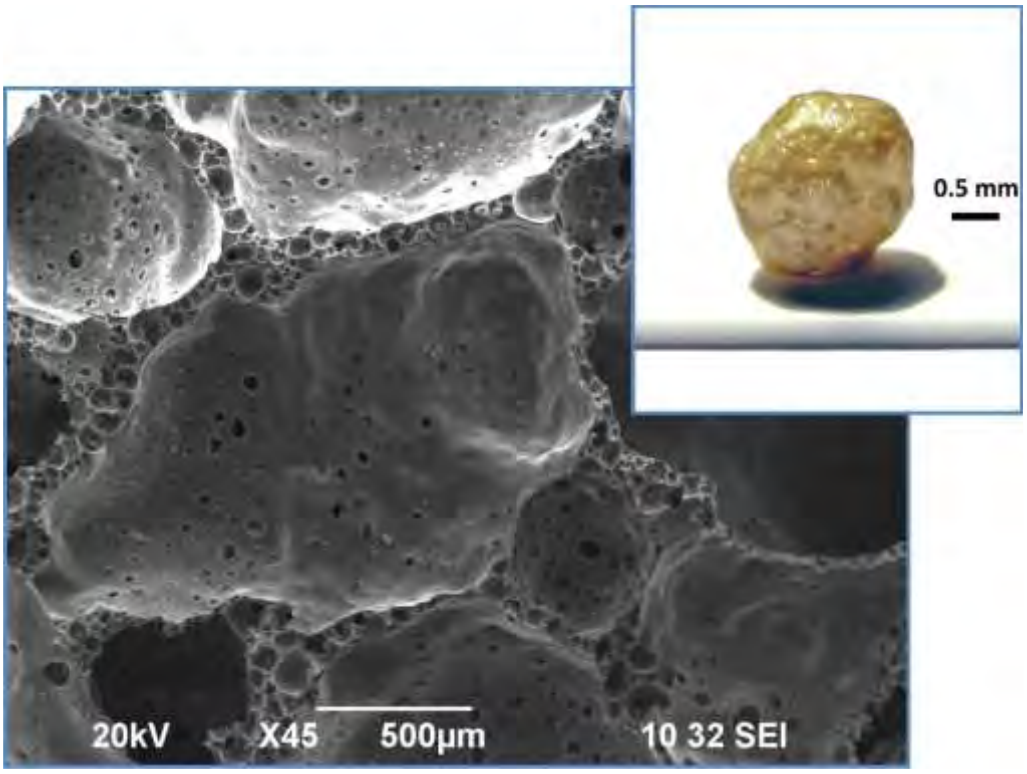


Figure 5. SEM image of a fracture surface of pyroxene glass-ceramic foam. Inset: color photograph of the external outline.

In our previous studies, we demonstrated that glass-ceramic foams similar to those investigated here precipitate crystalline phases—containing pyroxene crystals—in amounts of less than 30% [1, 7, 13].

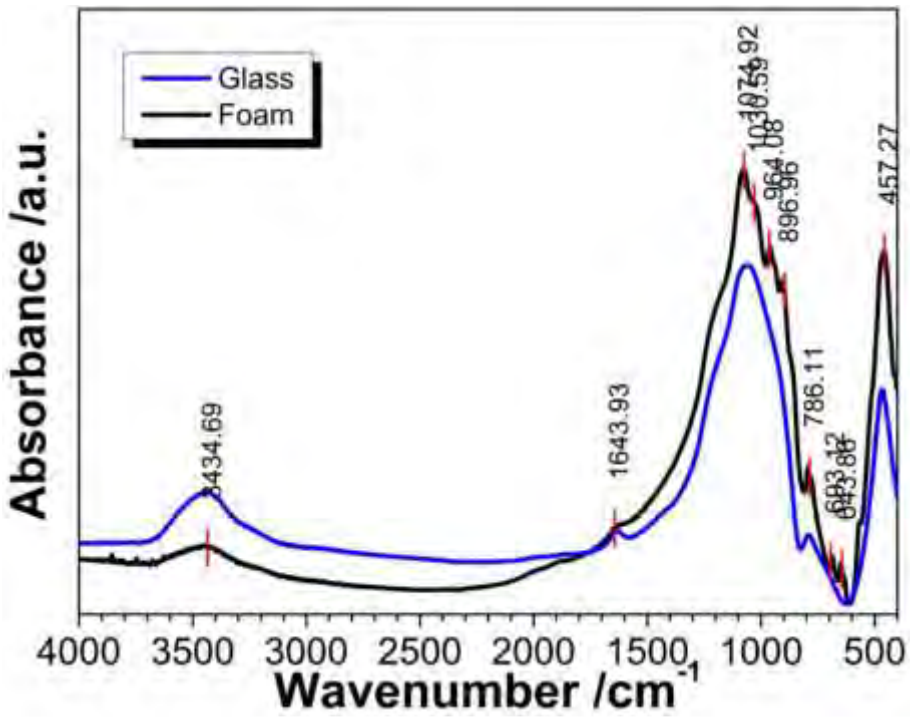


Figure 6. FT-IR spectra of a glass-ceramic foam (black) and the corresponding parent glass (blue).

Furthermore, the structure and chemical bonding of the newly obtained recycled glass-ceramic foams—compared with the parent glass—are illustrated via Fourier Transform IR spectroscopy of pressed samples prepared as sintered KBr matrix pellets.

The resulting infrared absorption spectra are relatively clean and simple, highlighting the presence of symmetric and antisymmetric siloxane (Si-O-Si) absorption bands at 1075 and 964 cm^{-1}, respectively; a calcium-oxygen band is observed at 897 cm^{-1}, along with Si-O deformation bands at 786 and 457 cm^{-1}.

.

These spectral characteristics can be attributed to diopside and wollastonite crystals, as shown graphically in Fig. 6. The assignment of the spectral bands is based on existing literature [14–16]. The IR spectrum of the parent glass shows no sharp peaks and reveals an amorphous nature.

To summarize the synthetic stages of a glass-ceramic foam, let us examine the following figure. Figure 7 illustrates in detail the formation of a glass-ceramic foam and all stages of thermal shaping within the temperature-induced volume change range: Figure 7a shows the initial state of the pressed specimen, with a snapshot taken at 700°C that is virtually identical to the starting sample. The densification process begins at approximately 800 °C, and the sintering of the glass-ceramics concludes at around 900 °C, as shown in Fig. 1b. Further heating up to 1050 °C resulted in no significant change in the sample volume. However, at this temperature, some smoothing of the shape was observed, followed by the onset of the foaming process. Furthermore, Fig. 1c illustrates the formation of a material characterized by a smooth, self-glazed surface, as this temperature is slightly above the softening point of the HM [17, 18].

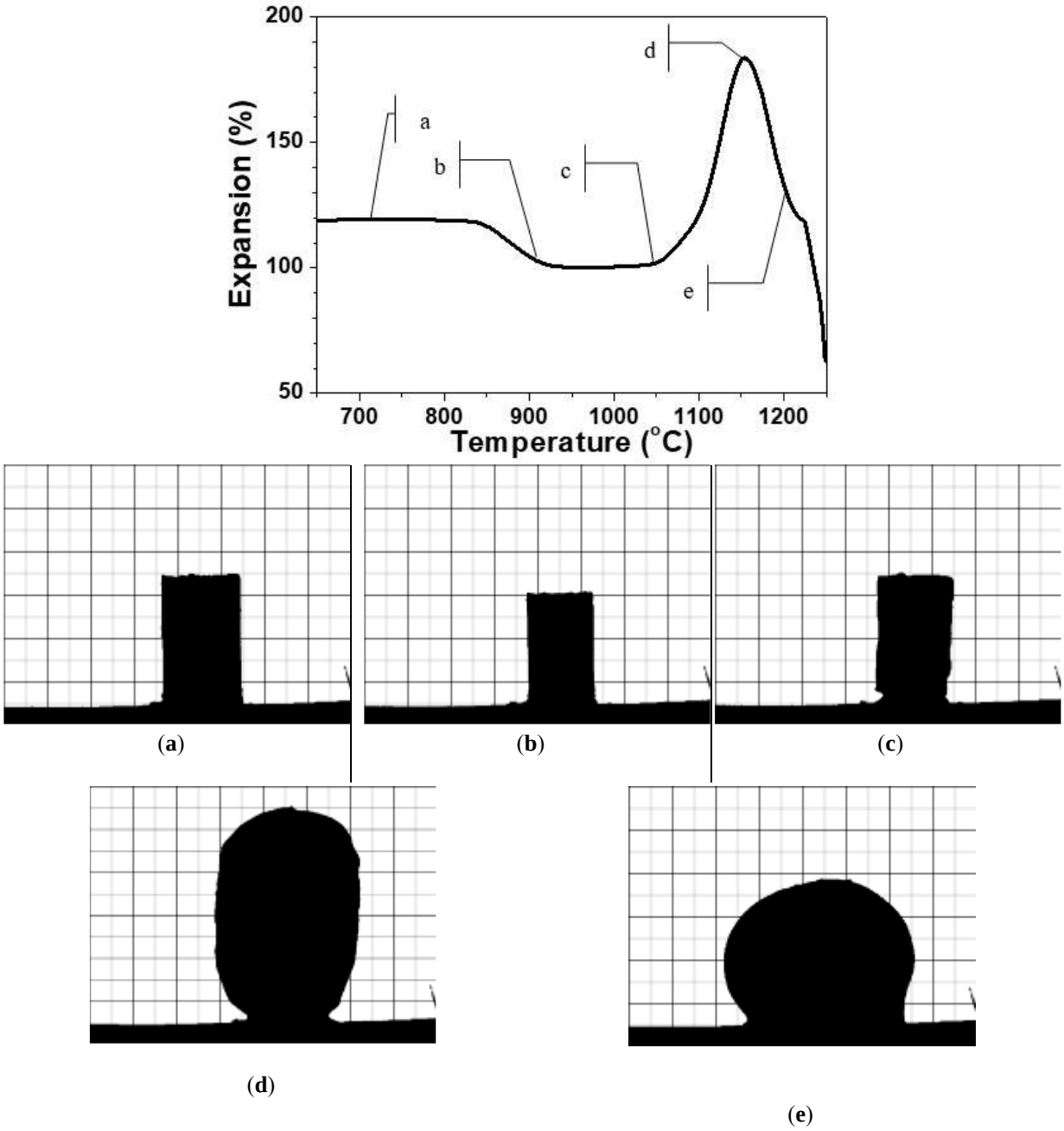


Figure 7. A lab volume change curve showing the sintering and expansion stages during the formation of a glass-ceramic foam. Silhouette images of the characteristic stages

of synthesis below.

Figure 7d shows the morphology at 1150°C, corresponding to the maximum degree of expansion during foaming. A further increase in temperature up to 1200°C, as shown in Fig. 7e, leads to rapid structural shrinkage and collapse of the foam.

The sample exhibits a nearly spherical profile (see Fig. 7e), indicating that at this temperature, gas evolution is complete and the apparent viscosity decreases due to the melting of crystalline phases formed during heating. This finding was established via DTA analysis in our previous work [19].

Figure 8 demonstrates results for "oxidized" and "non-oxidized" glass-ceramic samples obtained at a heating rate of 30 °C min^{-1}. As a result of the expected kinetic shift, the accelerated oxidation stage leads to a separation of the kinetic curves at higher heating rates, which in turn results in a more pronounced kinetic shift. Continuing the heating to 1050 °C, as shown in Fig. 8, initiates an autocatalytic foaming process. It is evident that foaming is more intense in the oxidized samples. Thus, the introduced oxidation step has actually led to an earlier onset of the foaming process. Pre-heat treatment practically ensures complete oxidation, which is a prerequisite for better foaming performance. This can be attributed to the presence of a higher content of Fe^{3+} ions in the oxidized samples, which is accompanied by earlier reduction and the release of oxygen molecules as the temperature rises.

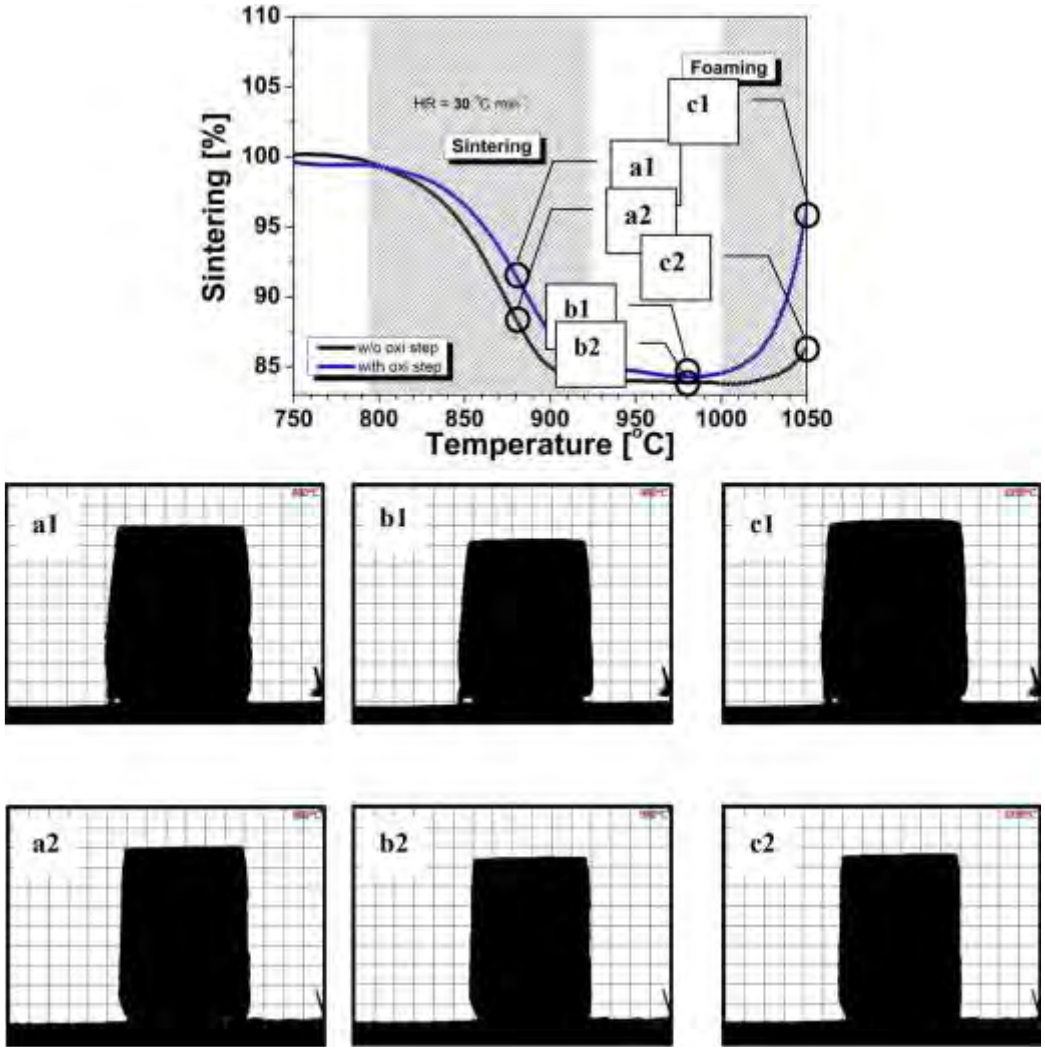


Figure 8. Sintering curves in TOS with an oxidation step (blue) and without an oxidation step (black). Representative images.

The silhouette images in Fig. 8 illustrate the change in shape during the formation of the new glass-ceramic material, achieved at a heating rate of 30 °C min^{-1}. Images captured via HM at the end of the sintering process (880 °C), at maximum shrinkage (990 °C), and at the onset of foaming (1050 °C) are presented in Figs. 8(a1–c1) and 8(a2–c2), respectively.

Additional experiments conducted at heating rates of 5 and 20 °C min^{-1} showed no significant differences.

For the purpose of a kinetic study of the sintering process, Fig. 9 presents a comparison of experimental sintering curves obtained at linear heating rates of 2, 10, and 30 °C min^{-1}, respectively. The curves were recorded during the *in-situ* sintering of glass-ceramics in air, using samples cut from a 5 cm parallelepiped. The finding that sintering improves with an increase in the heating rate is confirmed [20, 21].

At 950 °C (the temperature at which sintering is complete and the sintering rate is zero), we measured the following shrinkage values: 86.7% for 2 °C min^{-1}, 85.8% for 10 °C min^{-1}, and 84.7% for 30 °C min^{-1}.

As expected from general kinetic considerations—and indeed observed in experiments—the sintering range expands with increasing heating rate [22], a trend also observed in the present study. Here, the experimental curves shift toward higher temperatures as the heating rate increases, an effect most pronounced in samples measured at 2 and 10 °C min^{-1}. In addition, an interesting and unexpected observation was made regarding the sintering curves. Figure 9 shows a general overlap of the glass-ceramic sintering curves discussed—at heating rates of 10 and

30 °C min^{-1}—as is clearly evident from the figure. We hypothesize that one possible explanation for this effect is the insufficient time available for oxidation at the highest scanning rate. Furthermore, we anticipate that complete oxidation does not occur, which in turn leads to lower sample viscosity at 30 °C min^{-1}.

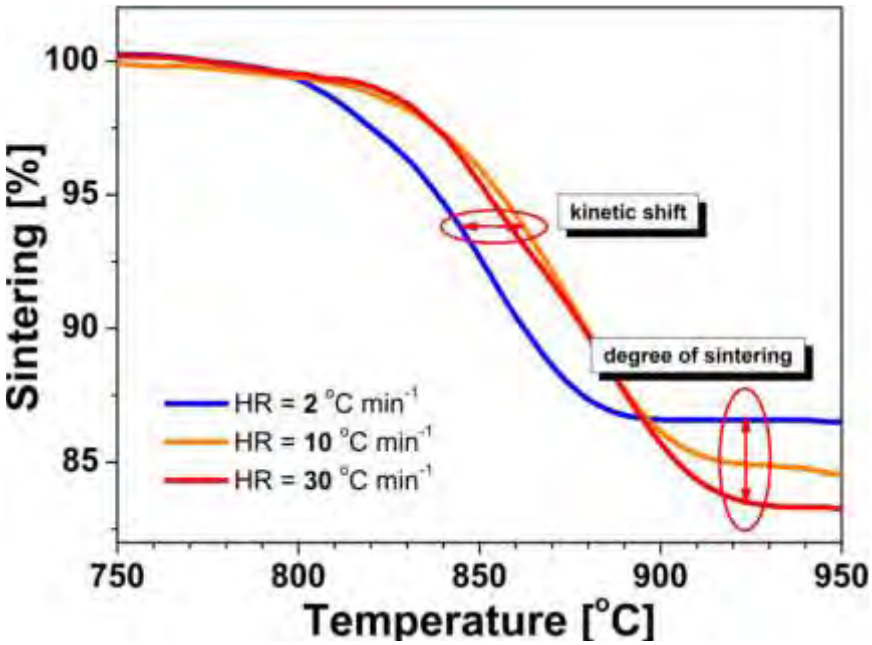


Figure 9. Sintering curves of glass-ceramic samples recorded at different linear sintering rates.

This decrease in viscosity is attributed to the presence of Fe^{2+} (ferrous) ions, which are known to act as modifiers within the glassy structural network. However, near the glass transition temperature (Tg), given sufficient time, the ions are expected to undergo complete oxidation to Fe^{3+} (ferric) ions; these act as network-forming oxides within the glassy structure, thereby increasing the viscosity.

We assume that somewhat similar behavior is also possible for the $Mn^{2+} \leftrightarrow Mn^{4+}$ redox couple [23].

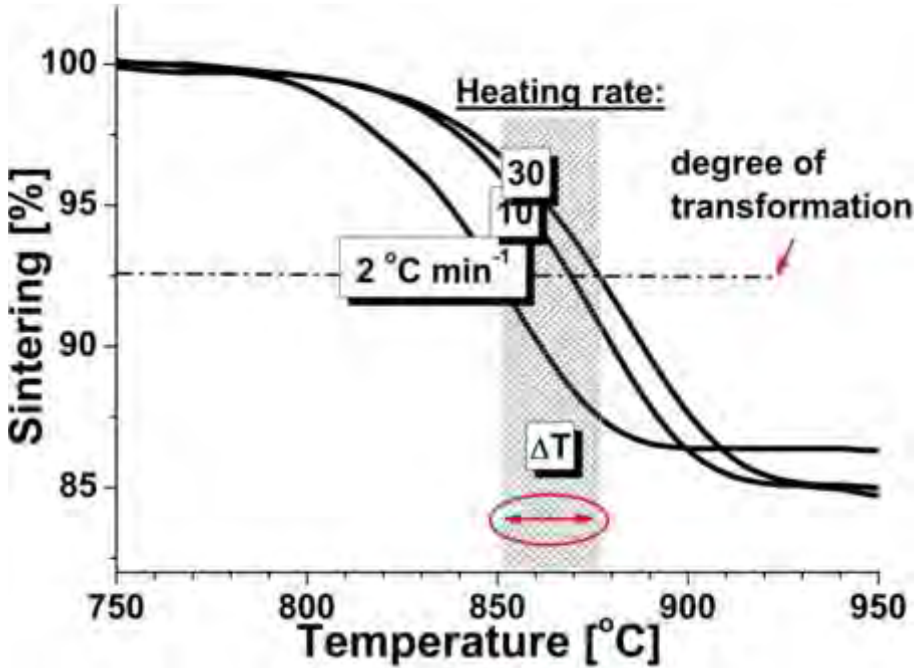


Figure 10. Kinetic analysis of the sintering process at three different heating rates and at a constant degree of conversion.

To elucidate this phenomenon, we introduced a preliminary isothermal oxidation stage—involving a 30-minute hold at 720°C in the glass transition region—prior to the sintering process during *in-situ* synthesis in a HM experiment [19]. Theoretically, sintering kinetics can be well approximated by a viscous flow process [24] and are described to a close approximation by the kinetic model developed by Cheng in [25], which is used here:

$$\frac{E_A}{RT} = ln\left(\frac{q}{T_X^2}\right) \quad (1)$$

where E_A [J mol^{-1}] is the activation energy for viscous flow, q [K min^{-1}] is the linear heating rate, and T_x [K] is the temperature at a fixed degree of transformation.
In our case, we use a fixed degree of transformation of 92.5% for all curves to perform the kinetic calculations (see the dashed line in Fig. 10).

To investigate the sintering kinetics, sintering curves were measured at heating rates of 2, 10, and 30 °C/min in both air and argon atmospheres. The results for argon are presented in Fig. 10. In an inert atmosphere, the oxidation of Fe^{2+} and Mn^{2+} ions cannot occur. In this specific case involving iron and manganese, the air and argon environments directly influence the sintering kinetics [23, 24].

In this case, no anomalies are observed in the kinetic behavior regarding the relationship between sintering temperature and heating rate. The experimental kinetic plots obtained for both air and argon atmospheres are presented in Fig. 11. The activation energy for sintering in air was determined to be E_A = 1020 J mol^{-1}, whereas the value in argon is lower, at E_A = 949 J mol^{-1}. Results showing similar activation energies can be found in other studies [22].

Despite the lower activation energies in argon, sintering in an inert atmosphere proceeds at lower temperatures. These features are attributed to the increased amounts of modifying F++ ions in the experiments conducted in an argon atmosphere.

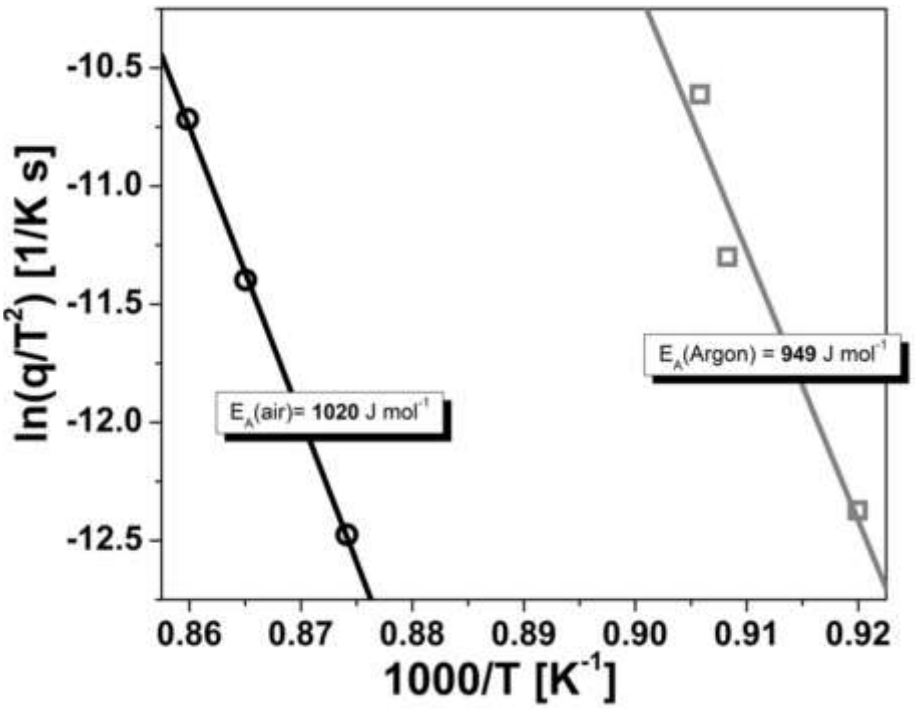


Figure 11. Kinetic analysis of Arrhenius plots.

To investigate the redox behavior in detail and elucidate the characteristics of the $Fe^{2+} \leftrightarrow Fe^{3+}$ and $Mn^{2+} \leftrightarrow Mn^{4+}$ couples in the synthesized glass-ceramics, samples were prepared and heat-treated in a furnace, followed by rapid air quenching after reaching the characteristic kiln temperatures.

It can be noted that quenching the melt to produce frit "freezes" (fixes) the equilibrium ratio of the Fe(II)/Fe(III) redox couple within the glass. In this instance, the ratio corresponds to the equilibrium value at the melting temperature.

However, oxidation occurs above the glass transition temperature. This effectively leads to the complete oxidation of Fe(II) to Fe(III). Upon further temperature increase, the reduction process resumes. It is interesting to note that when heat treatment is performed in an inert atmosphere, the oxidation and subsequent reduction associated with the formation of the glass phase are not observed.

Thus, by varying the temperature—and the associated changes in viscosity and redox processes—it becomes possible to obtain various sintered glass-ceramic materials.

V. Conclusions and contributions

In the present study, the authors demonstrated the feasibility of successfully synthesizing well-sintered glass-ceramics and/or glass-ceramic foams, depending on the temperature and the atmosphere employed. It was shown that synthesis in an inert atmosphere yields materials with a higher degree of sintering. With proper design, practical experience indicates that it is possible to obtain a glass-ceramic material with low density and high porosity—exceeding 85 vol. %—which can be considered a highly satisfactory result. Furthermore, the resulting foams exhibit fire resistance at temperatures up to 1100 °C.

By employing a double-stage heat treatment—comprising a first stage of low-temperature sintering at 950°C and a second stage of foaming at 1100°C—foam materials with improved properties and structural differences were successfully produced. SEM images of the fracture surfaces of both types of glass-

ceramic foam (produced in air and inert atmospheres) reveal a material that is satisfactorily sintered. They demonstrate a good degree of sintering and an overall porosity of less than 10–15 vol.%.

Inorganic materials produced via thermal foaming—such as those investigated in this study—can be used as modern construction materials and insulation products across various fields and industries, for instance, in the form of panels or custom-shaped components.

Generally speaking, inorganic glass-crystalline foam materials can be considered low-cost, lightweight materials with thermal insulation, sound insulation, and fire-resistant properties.

By varying the firing regime employed, we discussed and analyzed the possibilities for producing the following three types of materials: 1. sintered glass-ceramics; 2. self-glazed material; and 3. glass-ceramic foam.

The demonstrated processing flexibility is governed by thermal treatment rates and holding temperatures—due to variations in crystallinity and apparent viscosity—as well as by the tendency to bloat resulting from the thermal reduction of iron and manganese oxides present in the slag used.

At a heating rate of 10 °C min^{-1} and a heat treatment temperature of 950 °C, a well-sintered glass-ceramic is obtained, characterized by a bulk porosity of approximately 10 % and a moderate degree of crystallization—around 35 %.

Using higher heating rates (20 °C min^{-1}) and a short holding time at 1020 °C yields a product with a slightly deformed surface, characterized by self-glazing and a smooth, visually appealing finish.

Finally, heating rates in the order of 30 °C min^{-1} and holding at temperatures of 1100 °C enable the production of novel refractory sintered glass-ceramic foams with a cellular structure and a closed porosity of approximately 85–95 vol. %.

The ability to control open porosity could, for instance, enable the design of materials for filtration or catalysis applications.

The present research may contribute to a better understanding of the atmospheric influence on the synthesis of high-iron sintered and foamed glass-ceramic materials. It was highlighted that sintering activation energies and densification temperatures are lower in an argon atmosphere. The crystallization process is favored in argon, whereas the foaming process is favored in air.

In both sintered and foamed materials, the crystalline phases that form are pyroxene crystals present in varying amounts. To obtain accurate results for the sintering activation energies, a preliminary oxidation stage is required to ensure the complete oxidation of the samples. This oxidation process occurs near the glass transition region, whereas a thermal reduction process begins with a further increase in temperature.

An argon atmosphere completely inhibits foaming and improves the degree of sintering. Following an oxidation stage, foaming definitely occurs in both air and argon. It was noted that reduction—and consequently the foaming process—begins earlier in an inert atmosphere. In fact, higher Fe^{3+}/Fe^{2+} ratios in an inert atmosphere favor the early onset of the foaming process.

The kinetic effect is more pronounced in an inert atmosphere. Furthermore, we demonstrated that foam materials with varying structures can be obtained by employing a pre-oxidation step followed by synthesis in an argon environment.

Analysis of the isotherms indicates that the optimal heat treatment parameters are a temperature of 1120 °C and a holding time of 20 minutes. At lower isothermal treatment temperatures, the foaming process is incomplete, whereas shrinkage of the shape is observed at higher temperatures.

The moderate crystallinity and high porosity (85–95 vol. %) of the synthesized glass-ceramic foams determine the final properties of the recycled materials.

To reduce production costs, the effect of adding CaF_2 to the batch (2.5, 5, and 7.5 wt. %) on glass melting, densification, crystallization, and foaming was also investigated.

Increasing the CaF_2 content leads to a significant reduction in both melting and sintering temperatures. Furthermore, variations in the CaF_2 percentage, particle size fraction, heating rate, and holding temperatures alter sintering behavior, phase formation, and foaming capability.

Overall, the investigated glass powders (below 125 μm) exhibit good sintering characteristics in the 800–950°C range, followed by an intense foaming in the 1050–1150°C range.

Key contributions:

1. A unique closed vessel for operation in an argon atmosphere using a thermo-optical system (TOS) was designed for the first time, and the effect of the synthesis atmosphere on sintered glass-ceramic foams was demonstrated in detail.
2. Three types of materials were successfully obtained *in-situ* in the TOS through a sequential heat treatment series: highly densified glass-ceramics, autocatalytically glazed glass-ceramics, and glass-ceramic foam.
3. The sintering kinetics were investigated by recording sintering curves and applying an Arrhenius-type analysis method.
4. The redox nature of the synthesized materials and the influence of the oxidation state of transition metal oxides on the structure and properties of the final products were studied in detail.

References:

[1] Rincón A, Marangoni M, Cetin S, Bernardo E. Recycling of inorganic waste in monolithic and cellular glassbased materials for structural andfunctional applications. Journal of Chemical Technology & Biotechnology 91 (2016) 1946-1961. DOI: 10.1002/jctb.4982.

[2] Scarinci G, Brusatin G, Bernardo E. Glass foams. In: Scheffler M, Colombo P, editors. Cellular Ceramics: Structure, Manufacturing, Properties and Applications. Weinheim: Wiley-VCH; 2005. pp. 158-176. DOI: 10.1002/3527606696

[3] Sandrolini F, Palmonary P. Role of iron oxides in the bloating of vitrified ceramic materials. Transactions and Journal of the British Ceramic Society 75 (1976) 25-32.

[4] Petersen RR, Koenig J, Yue Y. The mechanism of foaming and thermal conductivity of glasses foamed with MnO2. Journal of Non-Crystalline Solids 425 (2015) 74-82. DOI: 10.1016/j.jnoncrysol.2015.05.030

[5] Chinnam RK, Francis AA, Will J, Bernardo E, Boccaccini AR. Review. Functional glasses and glass-ceramics derived from iron rich waste and combination of industrial residues. Journal of Non-Crystalline Solids 36 (2013) 563-574. DOI: 10.1016/j.jnoncrysol.2012.12.006

[6] Ovecoglu, M.L., Microstructural characterization and physical properties of a slag – based glass ceramic crystallized at 950 and 1000oC, J. Eur. Ceram. Soc. 18 (1998) 161–168.

[7] Khater, G.A., Influence of Cr2O3, LiF, CaF2 and TiO2nucleants on the crystallization behavior and microstructure of glass-ceramics based on blast-furnace slag, Ceram. Int. 37 (2011) 193–2199.

[8] C. Liu, Y. Shnip, D.Y. Zhang, M. Jiang, Development of glass ceramics made from ferrous tailings and slag in China, J. Iron Steel Res. 14 (2007) 73–78.

[9] Fiocco L, Elsayed H, Daguano JK, Soares VO, Bernardo E. Silicone resins mixed with active oxide fillers and Ca–Mg silicate glass as alternative/integrative precursors for wollastonitediopside glass-ceramic foams. Journal of Non-Crystalline Solids 416 (2015) 44-49. DOI: 10.1016/j.jnoncrysol.2015.03.001

[10] Karamanov A, Pelino M. Crystallization phenomena in iron rich glasses. Journal of Non-Crystalline Solids 281, 1-3 (2001) 139-151. DOI: 10.1016/S0022-3093(00)00436-1

[11] Karamanov A, Taglieri G, Pelino M. Sintering in nitrogen atmosphere of iron-rich glass-ceramics. Journal of the American Ceramic Society 87, 7 (2004) 1354-1357. DOI: 10.1111/j.1151-2916.2004.tb07734.x

[12] Jordanov, N.B., Kukeva, R., Stoyanova, R., Karamanov, A., Sinter-crystallization kinetics and foaming of glass from metallurgical slag in air and inert atmosphere, Thermochimica Acta 723 (2023) 179487, https://doi.org/10.1016/j.tca.2023.179487. ISSN: 0040-6031.

[13] Jordanov, N.B., Georgiev, I., Karamanov, A., Sintered glass-ceramics, self-glazed materials and foams from metallurgical waste slag, Materials 14 (2263) (2021),https://doi.org/10.3390/ma14092263, 1996-1944.

[14] Widjonarko, D.M., Jumina, J., Kartini, I., Nuryono, N., Phosphonate modified silica for adsorption of Co(II), Ni(II), Cu(II), and Zn(II), Indo. J. Chem. 14, 2 (2014) 143–151. DOI: https://doi.org/10.22146/ijc.21251, 2460-1578.

[15] Hussein, A.I., Ab-Ghani, Z., Che Mat, A.N., Ab Ghani, N. A., Husein, A., Ab. Rahman, I., Synthesis and characterization of spherical calcium carbonate nanoparticles derived from cockle shells, Appl. Sci. 10, 7170 (2020). DOI: https://doi.org/10.3390/app10207170, 2076-3417.

[16] Herth, E., Zeggari, R., Rauch, J.-Y., Remy-Martin, F., Boireau, W., Investigation of amorphous SiOx layer on gold surface for Surface Plasmon Resonance measurements, Microelectronic Eng. 163 (2016) 43–48. DOI: https://doi.org/10.1016/j.mee.2016.04.014, 1873-5568.

[17] Ljatifi, E.; Kamusheva, A.; Grozdanov, A.; Paunovi´c, P.; Karamanov, A. Optimal thermal cycle for production of glass–ceramic based on wastes from ferronickel manufacture. Ceram. Int. 2015, 41, 11379–11386.

[18] Agea-Blanco, B.; Reinsch, S.; Müller, R. Sintering and Foaming of Barium Silicate Glass Powder Compacts. Front. Mater. 2016, 3.

[19] Karamanov, A.; Hamzawy, E.M.; Karamanova, E.; Jordanov, N.B.; Darwish, H. Sintered glass-ceramics and foams by metallurgical slag with addition of CaF2. Ceram. Int. 2020, 46, 6507–6516.

[20] A. Karamanov, Vitrification and sinter-crystallization of iron-rich industrial wastes, Adv. Sci. Technol. 92 (2014) 174–183. DOI: https://doi.org/10.4028/www.scientific.net/AST.92.174.

[21] N.B. Jordanov, I. Georgiev, A. Karamanov, Sintered glass-ceramics, self-glazed materials and foams from metallurgical waste slag, Materials 14 (2021) 2263. DOI: https://doi.org/10.3390/ma14092263.

[22] A. Karamanov, B. Dzhantov, M. Paganelli, D. Sighinolfi, Glass transition temperature and activation energy of sintering by optical dilatometry, Thermochimica Acta 553 (2013) 1–7. DOI: https://doi.org/10.1016/j.tca.2012.10.006.

[23] R.R. Petersen, J. K¨onig, Y. Yue, The mechanism of foaming and thermal conductivity of glasses foamed with MnO2, J. Non-Cryst. Solids 425 (2015) 74–82.

[24] A. Karamanov, P. Pisciella, M. Pelino, The crystallisation kinetics of iron rich glasses in different atmospheres, J. Eur. Cer. Soc. 20 (12) (2000) 2233–2237.

[25] A. Karamanov, B. Dzhantov, M. Paganelli, D. Sighinolfi, Glass transition temperature and activation energy of sintering by optical dilatometry, Thermochimica Acta 553 (2013) 1–7, https://doi.org/10.1016/j.tca.2012.10.006.